

## Splash-cup plants accelerate raindrops to disperse seeds

Guillermo J. Amador, Yasukuni Yamada, Matthew McCurley and David L. Hu

*J. R. Soc. Interface* 2013 **10**,  
doi: 10.1098/rsif.2012.0880

---

### Supplementary data

["Data Supplement"](#)

<http://rsif.royalsocietypublishing.org/content/suppl/2012/12/12/rsif.2012.0880.DC1.html>

### References

[This article cites 29 articles, 4 of which can be accessed free](#)

<http://rsif.royalsocietypublishing.org/content/10/79/20120880.full.html#ref-list-1>

### Subject collections

Articles on similar topics can be found in the following collections

[biophysics](#) (209 articles)

### Email alerting service

Receive free email alerts when new articles cite this article - sign up in the box at the top right-hand corner of the article or click [here](#)



## Research

**Cite this article:** Amador GJ, Yamada Y, McCurley M, Hu DL. 2013 Splash-cup plants accelerate raindrops to disperse seeds. *J R Soc Interface* 10: 20120880. <http://dx.doi.org/10.1098/rsif.2012.0880>

Received: 27 October 2012

Accepted: 23 November 2012

### Subject Areas:

biophysics

### Keywords:

rain, projectile, seed dispersal

### Author for correspondence:

David L. Hu

e-mail: [hu@me.gatech.edu](mailto:hu@me.gatech.edu)

Electronic supplementary material is available at <http://dx.doi.org/10.1098/rsif.2012.0880> or via <http://rsif.royalsocietypublishing.org>.

# Splash-cup plants accelerate raindrops to disperse seeds

Guillermo J. Amador<sup>1</sup>, Yasukuni Yamada<sup>1</sup>, Matthew McCurley<sup>1</sup>  
and David L. Hu<sup>1,2</sup>

<sup>1</sup>School of Mechanical Engineering, and <sup>2</sup>School of Biology, Georgia Institute of Technology, Atlanta, GA, USA

The conical flowers of splash-cup plants *Chrysosplenium* and *Mazus* catch raindrops opportunistically, exploiting the subsequent splash to disperse their seeds. In this combined experimental and theoretical study, we elucidate their mechanism for maximizing dispersal distance. We fabricate conical plant mimics using three-dimensional printing, and use high-speed video to visualize splash profiles and seed travel distance. Drop impacts that strike the cup off-centre achieve the largest dispersal distances of up to 1 m. Such distances are achieved because splash speeds are three to five times faster than incoming drop speeds, and so faster than the traditionally studied splashes occurring upon horizontal surfaces. This anomalous splash speed is because of the superposition of two components of momentum, one associated with a component of the drop's motion parallel to the splash-cup surface, and the other associated with film spreading induced by impact with the splash-cup. Our model incorporating these effects predicts the observed dispersal distance within 6–18% error. According to our experiments, the optimal cone angle for the splash-cup is 40°, a value consistent with the average of five species of splash-cup plants. This optimal angle arises from the competing effects of velocity amplification and projectile launching angle.

## 1. Introduction

Splash-cup plants use specially shaped flowers (figure 1*a,b*) to harness the incoming kinetic energy of raindrops. An understanding of this mechanism has broad applications. Piezoelectric devices to harvest the kinetic energy of rain have been designed [1], and may benefit from a mechanistic understanding of splash-cup design. Ink-jet printing and industrial painting processes [2], which involve the high-speed deposition of drops onto a variety of small surface features, may also benefit from the insights of this study. Finally, understanding the interaction between plants and weather patterns such as rain, fog and dew has biological implications [3–5]. For example, the splashing of raindrops has been found to play a key role in foliar disease transmission [6]. Such interdisciplinary studies of the physical interactions between plants and rainfall may yield new insight into both the form of plants and the design of rain-resistant technology.

Splash-cup plants grow in a variety of locations, such as in tropical rain forests where regular rainfall occurs, and near waterfalls and mountain streams where splashing is common [7,8]. Under dense forests, even dewfall from overhanging trees is sufficient to trigger seed dispersal by splash-cup plants. In drier regions such as deserts, splash-cups plants are seasonal, relying on the rainy season to spread their seeds [7]. Regions of sparse vegetation are the most favourable surroundings for splash-cups, as they have the fewest obstacles to block the flying seeds [8].

The first observation of splash-cup seed dispersal was made by von Marilaun over a century ago in 1898 [9]. At that time, the high-speed camera had yet to be invented. Consequently, most splash-cup studies were purely observational, involving seed counts of the plants before and after a passing rain. Later, splash-cup plants were brought into the laboratory where their dispersal distance could be measured. Often such distances are striking: for

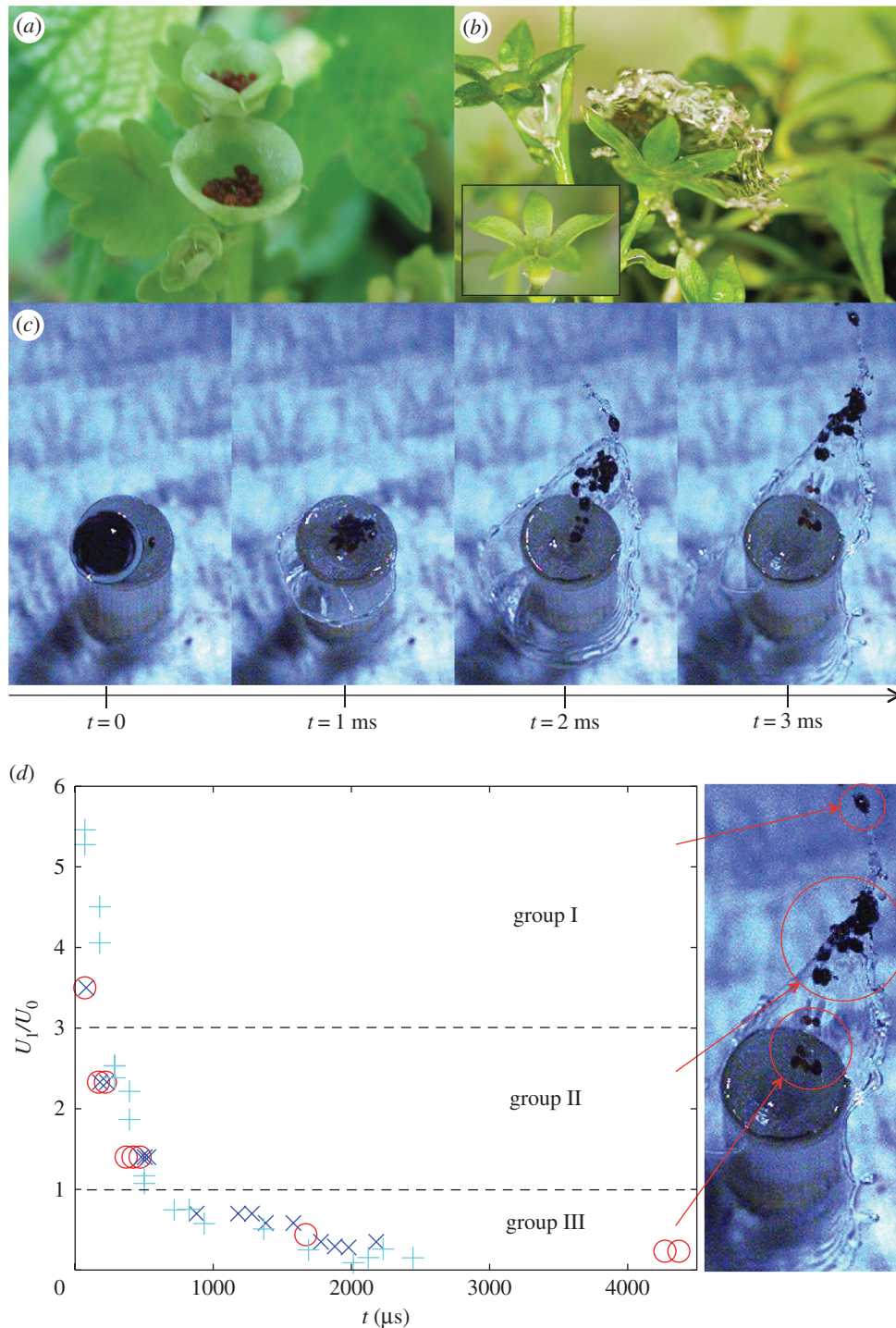


**Figure 1.** Splash-cup plants and their splashes. (a) The fruit body of *Chrysosplenium flagelliferum* filled with seeds. (b) The fruit body of *Mazus reptans* struck by a water drop. Inset shows the plan view of the fruit body. (c) Image sequence of an off-centre splash onto a splash-cup mimic. The mimic is filled with seeds from *Mazus reptans*. (d) Time course of velocity amplification  $U_1/U_0$  for three trials shown using the circle, cross and plus symbols, respectively. Time  $t = 0$  occurs when the drop first impacts the cone. (Online version in colour.)

example, *Chrysosplenium echinus* can disperse its 0.15 mg seeds horizontal distances of over 1 m, a distance equivalent to 10 plant heights [8]. Little explanation has been provided for these large distances. Biologists, like Nakanishi [8], have speculated that the unique geometry of the plants was responsible, but no physical model has been proposed. Saville in 1978 began studies of splash-cup physics with measurements of the relation between the size of raindrops and their terminal velocity which he inferred would influence the splash-cup's preferred habitat [10,11]. Saville's work remains the only quantitative study that attempts to link plant shape with the physics of raindrops.

In one of the most comprehensive works on splash-cup plants, Nakanishi characterized 19 splash-cup plant species in southern Japan [8]. He catalogued important physical parameters such as plant height, seed weight and quantity, and moreover performed simulated rain experiments to measure maximum seed dispersal distance. He observed that most splash-cups are 3–5 mm in diameter when mature [8], and noted that this closely coincided with the average diameter of raindrops, 2 mm (measured earlier by Saville [11]).

Although previous biological studies on splash-cups have focused on characterizing the dispersal distance of individual species, none have investigated the hydrodynamic mechanism

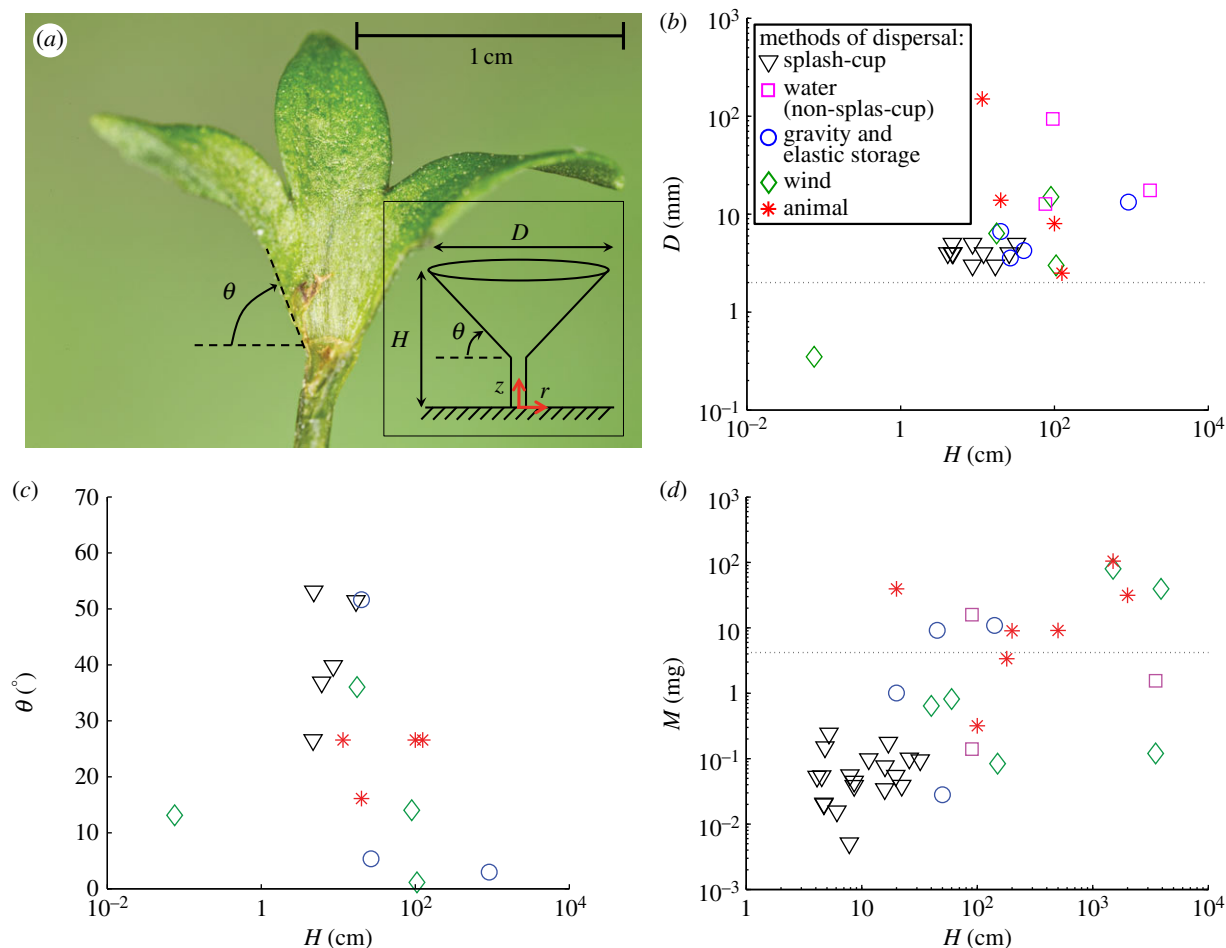


**Figure 2.** *Plant geometry.* (a) Cut-away view of splash-cup. Inset with a schematic showing geometric traits measured. (b) Relation between the fruit body diameter  $D$  and the plant height  $H$ . (c) Relation between the fruit body angle  $\theta$  and the plant height  $H$ . The horizontal line represents a 2 mm diameter of raindrops. (d) Relation between the seed mass  $M$  and the plant height  $H$ . The horizontal lines represent the masses of 2 mm diameter raindrops. Data were compiled from literature [8,14–57] and also from our own measurements. (Online version in colour.)

which allows this dispersal method to work so well. Furthermore, there have been no flow visualizations of drops impacting the splash-cup. In this interdisciplinary study, we attempt to ameliorate these gaps.

The hypothesis of our study is that the opening angle of the splash-cup fruit body is optimal for dispersing seeds across large distances. We will test this hypothesis using a series of high-speed video experiments as well as theoretical predictions for the splash speed and shape. In §2, we describe our experimental methods for building and filming splash-cup mimics, as well as our numerical methods for predicting dispersal distance. In §3.1, we compare the geometry of splash-cup plants with other plants, demarcating the range of variables we will consider in our parameter study. We present in §3.2 splash visualizations and experimental results for dispersal distance. We proceed in §3.3 with our presentation of mathematical model, and compare the results of this model to our experiments in §3.4. In §4, we discuss the implications of our work and suggest directions for future research; in §5, we close with our concluding remarks.

## 2. Material and methods

### 2.1. Plants

We procure splash-cup plants of species *Mazus reptans* from Woodlanders, Inc. They are raised indoors until their

flowers mature, leaving behind conical splash-cups (shown in figures 1*a,b* and 2*a*). Measurements of three different splash-cup plant species, *Mazus pumilus*, *Chrysosplenium japonicum* and *Sagina japonica*, are conducted in public parks in Southern Japan.

### 2.2. Plant mimics

Replicas of the conical fruit bodies of splash-cup plants are fabricated from UV curable resin using a three-dimensional printer (Objet Eden 250).

### 2.3. Measuring dispersal distance

We create rain by releasing 4 mm diameter drops from a 10 ml syringe. Our drop size represents the upper limit of raindrop sizes found in nature [11]. The syringe height of 35 cm dictates the drop speed of  $2 \text{ m s}^{-1}$ , which is less than raindrop terminal velocities ( $8\text{--}10 \text{ m s}^{-1}$  [12]). The experiments are conducted on a table covered with brown paper towels so that the secondary drops ejected from the splashes could easily be spotted.

As we show using dimensional analysis, our laboratory experiments produce dynamically similar splashes to those caused by falling rain. The splash of a drop onto a rigid surface is characterized by five physical variables: the drop diameter  $d$ , impact velocity  $U_0$ , liquid density  $\rho$ , viscosity  $\mu$  and liquid–gas surface tension  $\sigma$  [13]. Surface roughness and wettability

**Table 1.** Dimensionless groups and their values. For average rainfall, diameter  $d = 2$  mm and speed  $U_0 = 8$  m s<sup>-1</sup>.

dimensionless group	definition	rainfall	our experiments
Reynolds number	$Re = \rho d U_0 / \mu$	14,000	7000
Weber number	$We = \rho d U_0^2 / \sigma$	1800	220
Ohnesorge number	$Oh = \mu / \sqrt{\rho \sigma d}$	0.002	0.002

will be neglected in our analysis. This physical system may be characterized by several well-known dimensionless groups: this includes the Reynolds number, which relates inertial forces to viscous forces; the Weber number, which relates inertial forces to surface tension forces; and the Ohnesorge number, which relates viscous forces to surface tension forces. The respective associated dimensionless numbers for simulated rain and natural rain are given in table 1.

In both systems, Reynolds and Weber numbers are high, Ohnesorge number is low, and so inertial forces dominate over capillary and viscous effects. Thus, we conclude that our system is dynamically similar to raindrops at terminal velocity.

## 2.4. High-speed video of splash-shape

Visualizations of the splashes are obtained using a high-speed camera (Vision Research Phantom v. 9.0 and v. 720 with a Nikon AF Nikkor 50 mm/f1.8D macro lens). The splashes are filmed at 9280 frames per second. For visualization, 2 per cent of milk is used instead of water.

## 2.5. Satellite drop diameter measurement

Using high-speed video and particle-tracking software, we measure the relationship between cone angle and size of the satellite drops emerging from the splash. In figure 3c, we report the average diameters of the first five satellite drops to exit.

## 2.6. Film thickness measurement in off-centre impacts

To measure the thickness  $h$  of the film resulting from an off-centre drop impact, we used a slightly modified splash-cup with a small rod protruding halfway between the rim and the centre of the cup. A schematic is shown in the inset of the plot in electronic supplementary material, figure S1. The height of fluid along the rod is used to measure the thickness of the film. A series of experiments provides the film thickness at different positions  $\phi$  around the impact zone. The position  $\phi$  is shown schematically in the inset of electronic supplementary material, figure S1. The thinner film thicknesses occur for  $\phi$  ranging from  $-45^\circ$  to  $45^\circ$ , with the thinnest at  $\phi = 0^\circ$ . The location at  $\phi = 0^\circ$  is the location of interest.

## 3. Results

### 3.1. Regime diagrams for splash-cup geometry

In support of our hypothesis that splash-cup geometry leads to optimal dispersal distance, we determine regime diagrams for

plants that use different seed dispersal techniques. The data represent 50 plant species from the literature [8,14–57] along with our own measurements (of the species *Mazus pumilus*, *Chrysosplenium japonicum* and *Sagina japonica*) from public parks in Japan. In figure 2, we present height, diameter, opening angle and seed mass for each of these 50 plants. Tabulated values are given in the electronic supplementary material.

Splash-cup plants are generally short-statured, ranging in height from 4 to 30 cm, while other plants are generally over 40 cm in height. As initially suggested by Nakanishi, this stature prevents the seeds from blowing away by keeping them close to the ground where the wind is slowed by viscous boundary effects [8]. In our simulations, we will assume a constant plant height of 10 cm to predict dispersal distance.

Splash-cup plants have a variety of flower shapes, from cones to hemispheres to flowers with three or four petals. To compare sizes, we define  $D$  as the diameter of a disc with the same plan-view area as the flower. Figure 2b shows the effective diameter  $D$  of the splash-cup's fruit body compared to other plants. Splash-cups have small diameters, ranging from 3 to 5 mm, which closely corresponds to the 2 mm average diameter of rain drops, as stated in Nakanishi's previous work [8]. Non-splash-cup plants are generally larger in diameter, ranging up to 95 mm.

As we will show in the theoretical portion of our study, a critical parameter in determining the dispersal distance is the splash-cup's cone angle  $\theta$ . This angle is defined with respect to the horizontal, as shown in figure 2a. Figure 2c shows the opening angle for splash-cups compared with other plants. For splash-cups, the fruit body opening angle ranges from  $27^\circ$  to  $54^\circ$ , a relatively narrow range given their plant heights vary by an order of magnitude. Other kinds of flowers and fruit bodies are more variable, ranging from  $1^\circ$  to  $65^\circ$ , with the majority having lower opening angles than splash cups.

Lastly, splash-cup plants have much smaller seeds than other plants. Figure 2d shows that splash-cup seed masses  $M$  ranges from 0.005 to 0.180 mg, which is 1–4 orders of magnitude smaller than those of other plants, 0.03–105 mg. Splash-cup seeds are also lightweight compared with raindrops: the seeds are two orders of magnitude lighter than 2 mm diameter rain drops. On the basis of our measurements for the splash-cup-plant *Mazus miquelii*, the seed's material density of  $1719$  kg m<sup>-3</sup> is roughly 1.7 times that of water. The smallest drops ejected in the splash may be comparable in size to the seeds and so the mass of the seeds can indeed affect the distance achieved. For simplicity, we perform experiments with pure water striking empty splash-cups.

Based on our measurements of splash-cups, we manufacture splash-cup mimics according to the average shapes observed. To explore the effect of opening angle, we print eight cones at  $5^\circ$  increments of  $\theta$ , with opening angles ranging from  $30^\circ$  to  $65^\circ$ . Each cone has a diameter  $D$  of 5 mm, consistent with the average for splash-cup plants found by Nakanishi [8]. We place the cones at a height  $H$  of 10 cm from the ground, as defined in the inset of figure 2a.

## 3.2. Experimental results

### 3.2.1. Dispersal distance is sensitive to impact parameter

In his simulated rain experiments, Nakanishi observed a large variation (10–100 cm) of dispersal distances [8], but did not attempt to explain its cause. To investigate the cause

of this variation, we employ high-speed videography. By filming the impact of a drop onto our printed mimics while recording the maximum distance travelled by the ejected satellite drops, we made the discovery that the location of drop impact onto the cone greatly affects the dispersal distance of the drops.

Using high-speed films of 70 drop impacts, we categorized impacts into two types, on-centre and off-centre. We distinguish these types by defining a dimensionless impact parameter  $2\Delta r/D$ , where  $\Delta r$  is the horizontal distance between the centres of the drop and cone. On-centre impact corresponds to an impact parameter less than 0.2; off-centre impact corresponds to an impact parameter greater than 0.2. We found that this threshold of 0.2 led clearly to distinguishable splash shapes as shown by the insets in figure 3a. In particular, on-centre impacts result in splashes that are largely symmetric, with a ratio of maximum and minimum spread radii,  $R_{\min}/R_{\max} > 0.8$ , shown by the points in the upper left of figure 3a. Conversely, off-centre impacts generate splashes that are clearly asymmetric, associated with a radii ratio of 0.4–0.6, shown by the points in the lower right of figure 3a. As we will show, the shape of the splashes is indicative of different outgoing velocities and so dispersal distances.

Figure 3b shows the relation between dispersal distance and cone angle for 70 drop impacts performed in our laboratory. We distinguished the impacts into on or off centre based on the splash shape observed in high-speed video. This methodology results in repeatable measurements for dispersal distance, with low standard deviations between 3 per cent and 27 per cent. We clearly avoid the high variability observed by Nakanishi, who did not distinguish between the two impact types.

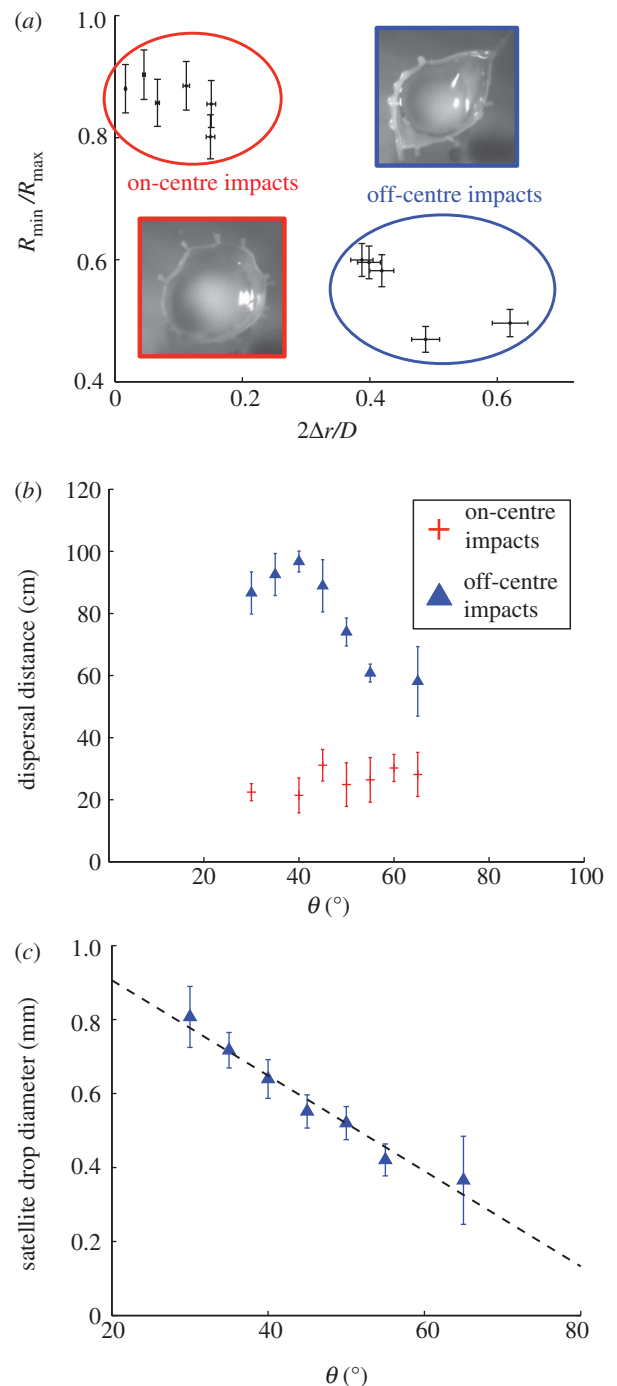
The on-centre impacts are shown by the crosses and the off-centre by the triangles. Clearly, off-centre impacts are the most effective in seeds dispersal, dispersing seeds to distances of 58–97 cm, or two to five times the distances of on-centre impacts, which disperse only to 21–31 cm.

Figure 3b shows trends consistent with the notion that splash-cups have an optimal geometry. In particular, off-centre impacts exhibit an optimal cone angle for maximizing dispersal distance. Dispersal distance at  $40^\circ$  is 97 cm, which is nearly double than that of  $65^\circ$  (58 cm) and 10 per cent higher than that of  $30^\circ$  (86 cm). On-centre impacts are less dependent on cone angle, showing only a slight increasing trend with the cone angle, increasing from 21 to 31 cm as cone angle increases from  $30^\circ$  to  $65^\circ$ .

### 3.2.2. Particle velocimetry in off-centre impacts

Once airborne, three parameters dictate dispersal distance: drop mass (which in turn affects drag coefficient), drop initial speed and initial trajectory angle. To quantify the initial speed of the farthest-dispersed seeds, we film three off-centre impacts on a splash-cup filled with 10–20 seeds. Figure 1d shows the time course of  $U_1/U_0$ , the launching velocity of seeds non-dimensionalized by the initial raindrop speed. The origin in figure 1d corresponds to contact between the incoming drop and the cup.

Raindrops are known for their height speed of 4–10 m s<sup>-1</sup>. Surprisingly, the exiting velocities of several seeds are greater than the incoming drop velocity. We categorize the seeds into three groups according to their velocity amplification.



**Figure 3.** Dispersal distance for the observed splash types. (a) The relation between dimensionless impact parameter  $2\Delta r/D$  and the ratio of maximum to minimum film radii. The error bars are based on the parallax error resulting from the camera not being perfectly overhead. (b) The relation between experimental dispersal distance and cone angle  $\theta$  for both on-centre and off-centre impacts. (c) The relation between the diameter of satellite drops and cone angle. (Online version in colour.)

The first group of seeds to exit the cup is group I, which has the highest velocity amplification of 3–5.5 times raindrop velocity and exits 70–300  $\mu$ s after drop impact. At times ranging from 300 to 500  $\mu$ s after impact the group II seeds exit, characterized by a velocity amplification ranging from 1 to 3. After 500  $\mu$ s, the last and slowest seeds, group III, exit with velocity amplifications of less than 1.

Even though group I has the largest velocity amplification, it comprises the fewest number of seeds, with the majority (90%) in groups II and III. For the remainder of

this investigation, we focus on rationalizing the 3–5.5 velocity amplification of the fastest seeds.

### 3.3. Modelling of splash profile and splash speed

We consider the hydrodynamics of impact onto inclined plates to rationalize the speed of the splash. Our modelling is two-dimensional and so flow in the azimuthal directions is neglected. We here derive relations for splash speed and, when possible, splash shape, paying particular attention to their dependence on cone angle. Readers interested only in comparisons between these derivations and our experiments may jump to §3.4.

#### 3.3.1. On-centre impact model

We apply a method introduced by Pasandideh-Fard *et al.* [58] to predict the splash speed of a drop striking the centre of a cone. Conservation of energy before and after the impact states  $KE_1 + SE_1 = SE_2 + W$ , which relates the kinetic and surface energies before ( $KE_1$  and  $SE_1$ ) and after impact ( $SE_2$ ) and the work  $W$  done against viscosity during the impact event. We estimate each of these energies in turn.

The total energy of an incoming water drop before impact consists of kinetic and surface energies, which are given by  $KE_1 = (\frac{1}{2}\rho U_0^2)(\pi/6)d^3$  and  $SE_1 = \pi\sigma d^2$ , respectively, where the associated variables are defined in §2.3. Following impact, the resulting thin film will grow radially before breaking into drops.

When the film has reached maximum extent, the surface energy is proportional to the surface area of the film, which can be discretized into four parts. These parts include: the free surface on top, the free surface underneath the film extending from the cone edge to the film edge, and the wetted surface area of the cone. The surface energy of the thin rim along the circumference of the film can be shown to be negligible using our measurement of the rim thickness (0.4mm) from high-speed video. Summing these surface areas, the total surface energy is  $SE_2 = 2\pi\sigma R_1^2/\cos\theta - \pi\sigma(D^2/4\cos\theta)(1 + \cos\theta_a)$ . Here  $\theta_a \approx 90^\circ$  is the contact angle between water and the cone surface (based on our measurements of contact angle for both the *Mazus reptans* and splash-cup mimic),  $\theta$  is the cone angle of the splash-cup, and  $R_1$  is the maximum spread radius of the film.

The viscous dissipation during the impact may be written  $W = \int_0^{t_c} \int_\Omega \phi d\Omega dt$  [58]; where  $t_c$  is the time it takes for the drop to spread (approximated as  $8d/3U_0$  [58]),  $\Omega$  the volume of the boundary layer and  $\phi$  the viscous dissipation function. Chandra & Avedisian [59] estimated the magnitude of  $\phi$  to be  $\mu(U_0/\delta)^2$ , where  $\delta$  is the boundary layer thickness of the film flow. This thickness,  $\delta$ , was found to be  $2(d/\sqrt{Re})$  by assuming that the fluid flow resembles symmetric stagnation point flow [58]. Using these results, the work against dissipation occurring in the boundary layer volume may be written as  $W = \frac{4}{3}\pi\rho U_0^2 d R_1^2 (1/\sqrt{Re})$ . Substituting these values into our original energy balance yields a quadratic equation which can be solved for the maximum spread radius of the lamella

$$R_1 = \sqrt{\frac{\rho U_0^2 d^3 + 12\sigma d^2 + 3\sigma(D^2/\cos\theta)}{24(\sigma/\cos\theta) + 16\rho U_0^2 d(1/\sqrt{Re})}}. \quad (3.1)$$

Using volume conservation with respect to the original drop volume yields an expression for the thickness  $h$  of the

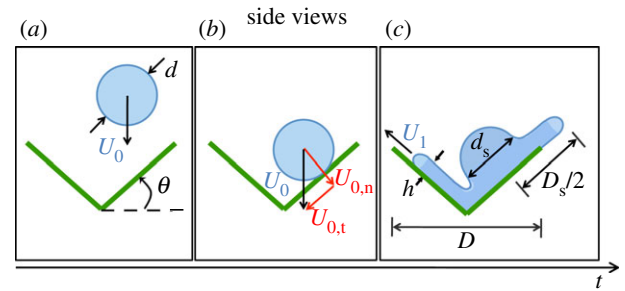


**Figure 4.** Velocity amplification mechanism for off-centre impacts (a–c) Time sequence of events during impact of a drop with a conical splash-cup. (a) Drop falls of diameter  $d$  falls with velocity  $U_0$ . (b) Touchdown occurs when the drop first contacts cone surface. The velocity  $U_0$  consists of two components,  $U_{0,n}$  and  $U_{0,t}$ , parallel and normal to the splash-cup surface, respectively. (c) During impact process, the splash creates a film of height  $h$  which exits the cup with velocity  $U_1$  in the left-handed direction. (Online version in colour.)

film:  $h = d^3/6R_1^2$ . Assuming a constant film thickness, we can approximate the spreading of the film as a spherical drop flowing into a flat, cylindrical film [58]. The volume flux out of the drop is  $(\pi/16)d^2 U_0$  and the volume flux of the spreading film is  $2\pi R_1 h U_1$ , where  $U_1$  is the spreading velocity. Conservation of mass states that these fluxes are equal, yielding an expression for the film velocity at maximum spread

$$U_1 = \frac{3U_0 R_1}{16d}. \quad (3.2)$$

Equation (3.2) provides splash speed of the drop, and so equivalently the initial speed of the encapsulated seeds as they begin their trajectory. To predict dispersal distance, we will apply our projectile motion equations presented in §3.3.3.

#### 3.3.2. Off-centre impact model

Consider a drop initially travelling at speed  $U_0$  striking a flat surface inclined at angle  $\theta$  with respect to the horizontal as shown in figure 4a. In this model, we consider impact upon a two-dimensional cavity rather than a three-dimensional cone. In both cases, the velocity amplification of the splash is because of the superposition of two effects arising from the physics of impact on an inclined surface. First, the drop has a component of its velocity which acts parallel to the inclined surface,

$$U_{0,t} = U_0 \sin\theta, \quad (3.3)$$

as shown in figure 4b. Second, when the drop strikes the surface, the resulting spreading film will add momentum to the already moving frame of the drop.

We consider in greater detail the contribution from film spreading by applying conservation of mass during impact, as first done by Pasandideh-Fard *et al.* [58]. During impact, the spherical drop is transformed into a truncated sphere of width  $d_s$  that flows into a thin, cylindrical, expanding film of height  $h$  and diameter  $D_s$ , as shown in figure 4c. Applying mass conservation for the flow rates between the spherical section and the rim of the film yields an expression of the velocity  $U_s$  at the edge of the film

$$U_s = \frac{d_s^2}{4D_s h} U_{0,n}, \quad (3.4)$$

where  $U_{0,n} = U_0 \cos \theta$  is the component of the drop velocity striking the surface normally, as shown in figure 4*b*. We use high-speed video experiments to estimate the length scales  $d_s$ ,  $D_s$  and  $h$  for a single cone of  $45^\circ$ . We assume that these measurements remain valid across the range in cone angles studied ( $30^\circ$ – $65^\circ$ ). In support of this assumption is a previous study by Šikalo *et al.* [60] which found that the spreading velocity for film resulting from an impact of a drop onto an inclined surface was independent of the incline angle at short timescales after impact.

In our experiments, we observed that the variables  $d_s$ ,  $D_s$  and  $h$  will evolve throughout the duration of impact as the drop travels downward. For our modelling, we choose to measure these variables when the maximum film spread  $D_s$  is equal to twice the slant height of the cone  $D/\cos \theta$ , as shown in figure 4*c*. At that moment, the total velocity of the resulting splash of a drop on an incline is a sum of equations (3.3) and (3.4),

$$U_1 = U_0(\sin \theta + \alpha \cos \theta), \quad (3.5)$$

where the parameter  $\alpha = d_s^2 \cos \theta / 4Dh$ . Based on our measurement method in §2.6 we find:  $h \approx 0.3$  mm,  $D_s \approx 7$  mm, and  $d_s \approx 4$  mm. Thus, we find a characteristic value for  $\alpha = 2$ . We will use this value of  $\alpha$  in theoretical predictions for splash speed and dispersal distance.

### 3.3.3. Predicting dispersal distance

We predict the dispersal distance of seeds using well-known equations of projectile motion for high-Reynolds number drag on raindrops. The projectile we simulate is the seed of *Sagina japonica* encapsulated within a satellite drop of water exiting the splash after impact. The mass  $m$  of these drops are found in our experiments. The tabulated drag coefficient for drops of mass  $m$  at terminal velocity is taken from Gunn [12]. The seed launching angle is simply the splash-cup opening angle  $\theta$ , shown in figure 2*a*. The initial velocity of the seed is derived from theory in §§3.3.1 and 3.3.2.

We define the origin for calculating dispersal distance in the inset of figure 2*a*. The initial position of the drop when exiting the cup is given by the cup's geometry: the initial height of the drop is  $H$  and the radial position is  $D/2$ , where  $D$  is the diameter of the splash-cup as shown in the inset of figure 2*a*. Drops travel radially in the  $r$ -direction and rise and ultimately fall in the  $z$ -direction. The following accelerations in the  $r$ - and  $z$ -directions are numerically integrated in MATLAB to find the dispersal distance

$$a_r = -\frac{1}{2} \frac{\pi \rho_a d^2 C_D}{4m} U^2 \cos \theta \quad (3.6)$$

and

$$a_z = -g - \frac{1}{2} \frac{\pi \rho_a d^2 C_D}{4m} U^2 \sin \theta. \quad (3.7)$$

Here,  $\rho_a$  is the density of air,  $g$  the acceleration due to gravity,  $C_D$  the drag coefficient,  $m$  and  $d$  are the drop mass and diameter,  $U$  is its velocity and  $\theta$  is the angle of direction with respect to the horizontal. For integration, we use a first-order scheme and an infinitesimal time step of  $10^{-6}$  s. We used an initial height  $H$  of 10 cm, the value used in our experiments in §3.2.

## 3.4. Comparison of experiments to theory

### 3.4.1. On-centre impacts

Figure 5*a,b* shows an on-centre impact onto the splash-cup. An image sequence and computer illustration is shown for clarity. Upon impact, the resulting film spreads along the surface of the splash-cup in a distinctly circular lamella. This lamella increases in radius until reaching a maximum of  $R_1$  before breaking up at time  $t = 6.6$  ms.

Figure 5*c* shows the relation between the maximum spread radius  $R_1$  and drop impact velocity. Over the range of impact velocities from 2.2 to 2.8  $\text{m s}^{-1}$ , the spreading radii in our experiments, shown by the crosses, increases from 6 to 8 cm. The dashed line in this figure corresponds to the theory from equation (3.1), which predicts spread radii values increasing from 7.1 to 8.6 cm over this range of impact velocity. These predictions are excellent for the highest drop speeds at 2.7  $\text{m s}^{-1}$ , and for the remaining speeds are accurate within 25%. Note that our model was able to come to this precision without the use of free parameters but only relying upon the initial speeds and sizes of the drop and the shape of the cone.

We use our model to gain insight into the effect of cone angle on dispersal distance. Previously, we saw in our experiments (the crosses in figure 3*b*) that dispersal distance for on-centre impacts was quite low, and nearly independent of cone angle. The reason for this poor dispersal distance is now made clear by our model, which considers two effects occurring in sequence. First is the effect of the cone angle on the exiting velocity of the splash. Second is the effect of cone angle on the trajectory of the drop. The dispersal distance results from a combination of these effects, which we consider in turn.

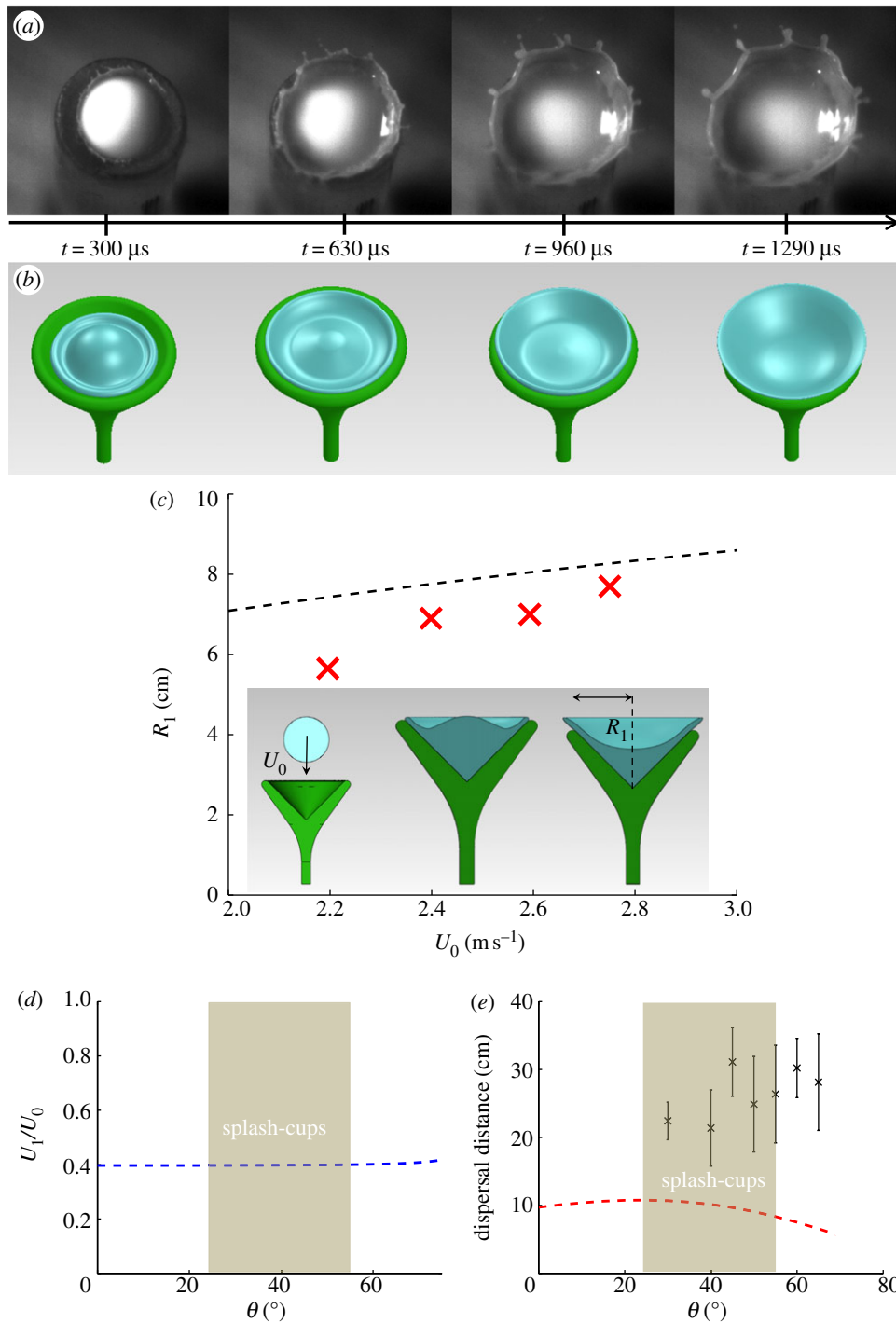
Figure 5*d* shows the predicted relation between cone angle and the dimensionless exiting velocities of the splash. The region of interest in this figure is the region marked in brown, which refers to the cone angles of  $25^\circ$ – $55^\circ$  observed among splash-cup plants. Clearly, the dimensionless splash velocity is low, with values of 0.4–0.41, which are nearly invariant as a function cone angle. Thus, on-centre impacts result in splashes that decelerate the drop and so create poor initial conditions for dispersing seeds.

Figure 5*e* shows the relation between cone angle and dispersal distance. Black crosses indicate experimental results. The dashed line is the theoretical prediction which uses projectile motion equations to combine the measured drop masses (see §2.5), the predicted initial velocity of the drops presented in figure 5*d*, and the initial angle of the trajectory given by the cone angle. The predicted dispersal distance is quite low, 8–12 cm. This range under-predicts the experimental values by up to 40 per cent for the  $65^\circ$  cone, as shown by the relative positions of the crosses and dashed line in figure 5*e*.

For on-centre impacts, we predict dispersal distance peaks at  $20^\circ$ . This is because of the combination of a relatively constant exiting velocity and the effects of cone angle on drop trajectory, of which the latter is primarily responsible for producing this peak. Nevertheless, the dispersal distances for this type of impact are so low that on-centre impacts are poor methods for dispersing seeds.

### 3.4.2. Off-centre impacts

Off-centre impacts create almond-shaped splashes as shown in figure 6*a,b*. The emerging lamella becomes increasingly sharp because of the film spreading at a faster rate in the



**Figure 5.** *On-centre splash.* (a,b) Time sequence of a drop striking a  $45^\circ$  cone on-centre, shown using high-speed video (a) and computer illustration (b), given for the sake of clarity. (c) Relation between maximum film spread radius  $R_1$  and drop initial velocity  $U_0$ . The crosses represent the experimental data and the dashed line the theoretical prediction. Inset shows computer illustration of side-view of an on-centre splash. (d) The relation between velocity amplification and cone angle. (e) The relation between theoretical dispersal distance and cone angle. Experimental data by the black crosses and theoretical predictions by the dashed line. The shaded regions of the plots represent the range of cone angles found for splash-cup plants. (Online version in colour.)

direction of maximum velocity amplification. This direction is on the line defined by the centres of the drop and cone. A side view of the splash, shown in figure 6c,d, shows the asymmetric spread of the exiting thin film more clearly. In particular, the rapidly elongating jet in figure 6c indicated the direction of greatest velocity amplification.

We now compare quantitatively our predictions and experiments for splash velocity and dispersal distance. In our particle-tracking experiments (figure 1d), we found that the maximum dimensionless exiting velocities of seeds varied from 3 to 5.5. Using our theory in equation (3.5), the

corresponding dimensionless velocity is 2.1 for a  $45^\circ$  cone, as shown in figure 6e. This theory under-predicts experimental values by 25–50%. Nevertheless, it captures our theory's striking factor of two to five difference in velocity between on-centre and off-centre impacts.

Using our theory, we can easily infer the effect of cone angle on exiting drop velocity. For the range of splash-cups observed, we predict that dimensionless exiting velocities will range from 1.8 to 2.2. Thus, it is clear that off-centre impacts are effective means of seed dispersal as they accelerate the already high speeds of falling raindrops. According to

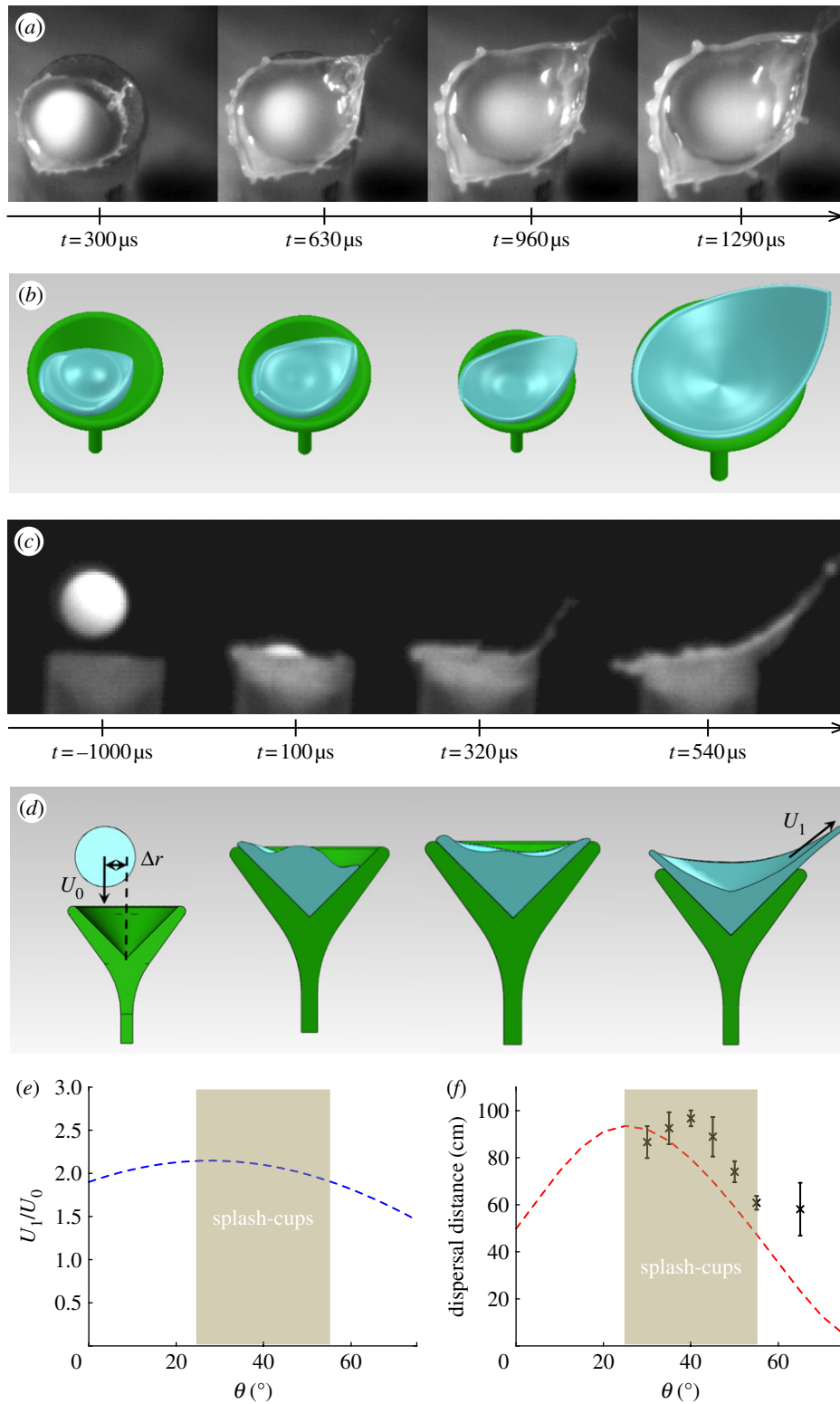


**Figure 6.** *Off-centre splash.* (a,b) Plan-view time sequence of an off-centre drop impact, shown using high-speed video (a) and computer illustration (b). (c,d) Side-view time sequence of the drop impact. In (a–d), a  $45^\circ$  cone is shown. (e) The relation between velocity amplification and cone angle. (f) The relation between dispersal distance and cone angle. Experimental data are given by the black crosses and the theoretical prediction is given by dashed line. The shaded regions of the plots represent the range of cone angles found for splash-cup plants. (Online version in colour.)

our theory, peak velocity amplification occurs at cone angles of  $30^\circ$ .

Figure 6f shows the relation between cone angle and dispersal distance for off-centre impacts. Experiments are given by black crosses and theory by the dashed line. The model incorporates the combined effects of velocity amplification, decrease in satellite drop diameter as measured in the experiments in §2.5 and the effect of cone angle on particle

trajectory. Generally, the model is quite good and predicts values within 6–18% our experiments, as shown as the black crosses in figure 6f. The prediction of an optimal cone angle is qualitatively correct, predicting a value of  $25^\circ$ , which is 37 per cent less than our experimental value of  $40^\circ$ .

Both our experiment and theory show that off-centre impacts are an excellent means to disperse seeds. As shown from the experimental data figure 3b and the theoretical

data in figures 5e and 6f, the off-centre dispersal distances are roughly two to five times larger than those resulting from on-centre impacts.

## 4. Discussion

### 4.1. Limitations of our model

Our study yields new insight into the optimal cone angle for splash-cup plants, found to be  $40^\circ$  using high-speed splash experiments and measurements of splash-cup plants. Using theory, we found that this peak arose from a combination of effects stemming from the splash-cup's opening angle. In particular, opening angle affects the velocity amplification, the size of the secondary drops and their launching angle. Thus, the cup's opening angle affects both the hydrodynamics of drop impact and aerodynamics of particle motion. The subtleties involved thus may suggest why splash-cups generally have a range of opening angles. These angles may be influenced by factors we did not consider such as deviations in the cup shape from a cone, the cup's surface wettability and inter-species variation in the size and shape of their seeds.

Our theory is not applicable for nearly horizontal surfaces, for which no amplification should occur. Breakdown of our theory occurs because the parameter  $\alpha$  was only measured for a cone of  $45^\circ$ . Studies of splashes on horizontal surfaces generally assume no velocity amplification. Exceptions exist for a small amount of fluid at the very beginning of the splash, for which an amplification of 1.6 has been observed [61]. This amplification effect is not well understood. However, it is probably not pertinent to our study of splash-cups, as the amplification of 1.6 is much smaller than the factor of three to five observed in our experiments for off-centre impacts.

### 4.2. Optimal opening angles for horizontal and vertical dispersal

We note that our optimal angle of  $40^\circ$  disagrees with Brodie's previous conjecture that the most efficient splash-cups have opening angles of  $60^\circ$ – $70^\circ$  based upon his observations of the bird's nest fungus which has an opening angle of  $60$ – $70^\circ$  [62]. Brodie's result is not inconsistent with our own. Instead, the systems he studied are probably focused on vertical rather than horizontal dispersal: the splashes on bird's nest fungus serve to shoot tendrils at the maximum height in order to reach taller plants [62]. Plants that shoot for vertical dispersal will indeed have higher optimal angles. According to our preliminary calculations, vertical dispersal distance for splash-cups is maximized at an angle of  $50^\circ$ . Thus, the methods in this study may find use in finding optimal plants shapes for other kinds of spore and seed dispersal.

### 4.3. Splash-cup seed dispersal among other plants

The effective splashes observed in this study may also be observed in other plants similar in shape to splash-cups. In our study, we found that cone angle has the greatest influence on velocity amplification and so splash effectiveness. The regime diagram in figure 2b shows that certain other plants have cone angles near  $40^\circ$ , the optimal angle for splash-cup

seed dispersal. In particular, two plants that use wind to disperse their seeds, *Chimaphila maculata* and *Viola arvensis* Murray, have cone angles of  $36^\circ$  and  $51^\circ$ , respectively. We hypothesize that these two plants would be able to use rain to disperse their seeds as well, if their seeds were appropriately sized. The evolution of these plants is consistent with our hypothesis: Nakanishi speculates that splash-cup plants evolved from species that use wind-seed dispersal [8].

Splash-cup seed dispersal is not generally used among all plants, however. As mentioned previously, most plants have seeds too large to be encapsulated in raindrops. Moreover, many plants have nearly flat fruit bodies, with cone angles near  $0^\circ$ . For example, *Sisymbrium altissimum* and *Erythrina variegata* have cone angles of  $1^\circ$  and  $3^\circ$ , respectively. Such plants would have little or no velocity amplification according to our theory: instead such impacts would resemble the well-studied impact onto a horizontal surface.

### 4.4. Off-centre impacts most likely

In a rainstorm, drops fall at all positions with uniform probability; consequently, a range of dispersal distance is to be expected in nature. Thus, Nakanishi's finding of a range of dispersal distances is likely comparable to those found in the field. Nevertheless, we can comment on which kinds of impacts are most probable, and thus most contributing to the natural selection of the plant.

Given a splash-cup whose plan view shape is that of a unit disk, on-centre impacts will occur within a disk of radius 0.2, which has an area of  $0.04\pi$ . Off-centre impacts occur in the remaining annulus, which has an area of  $1 - 0.2^2\pi = 0.96\pi$ . Thus, the ratio of these areas are  $0.04/0.96 = 0.04$ . Thus, off-centre impacts 24 more times probably than on-centre impacts. This probability combined with the much greater effectiveness of off-centre impacts indicates that off-centre impacts are most probably involved in natural selection.

### 4.5. Flexibility of splash-cup plants

In our experiments we used splash-cups held rigidly in place. In reality, the flexible stem of the fruit body causes it to oscillate when struck by a water drop. This creates a spring-like effect, which in our experiments seemed to hinder the splash-cup's performance. Thus, it remains unknown why splash-cup plants are so flexible. We hypothesize that the effect on the drop could be similar to that observed in the transmission of foliar disease in plants by rain [6].

## 5. Conclusion

We have presented a hydrodynamic mechanism for the seed dispersal of splash-cup plants. We found two variables that greatly influence dispersal distance. The first is the impact parameter, the horizontal distance between the centre of the cup and the incoming drop. We used the impact parameter to distinguish between on and off-centre impacts. Thus, off-centre impacts are most effective for maximizing dispersal distances and are thus most likely to be involved in natural selection of the plant.

The second variable affecting seed dispersal is the cone angle, which we hypothesized was optimized to yield maximum splash distance. We tested this hypothesis using a combination of splash-cup plant measurements, high-speed

video experiments and hydrodynamic theory. Experiments and theory each showed that splash-cup plants should have opening angles of 40° to maximize distance. Dispersal distances of seeds can reach nearly 1 m from the cup, quite a long distance given the height of the cup (approx. 10 cm on average).

The primary mechanism for achieving large dispersal distances is the creation of fast splashes. In experiments, we found raindrops are accelerated by a factor of 3–5 in speed during impact with a splash-cup. Our theory showed that this anomalous velocity amplification results from the combination of two sources of momentum, the component of the drop's initial velocity parallel to the cup's inclined wall, and the resulting film spread owing to the impact of the

drop with the wall. Using this theory, we predicted a velocity amplification of 2, and predicted the drop's dispersal distance to be within 6–18% of the observed values.

The splash-cup's method of creating fast splashes is novel, as traditionally studied splashes on flat surfaces do not result in amplification of speed [58,59,61]. This velocity amplification concept may find application to other types of conical surfaces found in the natural world, such as flowers and leaves, and in technological applications seeking to either maximize or minimize splashing.

The authors thank the Georgia Tech Invention Studio for providing equipment for three-dimensional printing and the NSF (PHY-0848894) for financial support.

## References

- Guigon R, Chaillout J, Jager T, Despesse G. 2007 Harvesting raindrop energy: experimental study. *Smart Mater. Struct.* **17**, 015039. (doi:10.1088/0964-1726/17/01/015039)
- Bakshi S, Roisman I, Tropea C. 2007 Investigations on the impact of a drop onto a small spherical target. *Phys. Fluids* **19**, 032102. (doi:10.1063/1.2716065)
- Roth-Nebelsick A *et al.* 2012 Leaf surface structures enable the endemic namib desert grass *Stipagrostis sabulicola* to irrigate itself with fog water. *J. R. Soc. Interface* **9**, 1965–1974. (doi:10.1098/rsif.2011.0847)
- Vogel S, Müller-Doblies U. 2011 Desert geophytes under dew and fog: the curly-whirlies of Namaqualand (South Africa). *Flora-Morphol. Distrib. Funct. Ecol. Plants* **206**, 3–31. (doi:10.1016/j.flora.2010.01.006)
- Vogel S. 1989 Drag and reconfiguration of broad leaves in high winds. *J. Exp. Bot.* **40**, 941–948. (doi:10.1093/jxb/40.8.941)
- Gilet T, Bourouiba L, Bush J. 2011 Foliar disease transmission: insights from fluid dynamics. In *APS division of fluid dynamics Meeting Abstracts*, vol. 1, p. p16001. College Park, MD: American Physical Society (APS).
- Parolin P. 2006 Ombrohydrochory: rain-operated seed dispersal in plants—with special regard to jet-action dispersal in Aizoaceae. *Flora-Morphol. Distrib. Funct. Ecol. Plants* **201**, 511–518. (doi:10.1016/j.flora.2005.11.003)
- Nakanishi H. 2002 Splash seed dispersal by raindrops. *Ecol. Res.* **17**, 663–671. (doi:10.1046/j.1440-1703.2002.00524.x)
- von Marilaun AK. 1898 *Pflanzenleben: Bd. Die Geschichte der Pflanzen*, vol. 2, Gotha, Germany: Bibliographisches institut.
- Savile D. 1953 Splash-cup dispersal mechanism in *Chrysosplenium* and *Mitella*. *Science* **117**, 250. (doi:10.1126/science.117.3036.250)
- Savile D, Hayhoe H. 1978 The potential effect of drop size on efficiency of splash-cup and springboard dispersal devices. *Can. J. Bot.* **56**, 127–128. (doi:10.1139/b78-014)
- Gunn R, Kinzer G. 1949 The terminal velocity of fall for water droplets in stagnant air. *J. Atmos. Sci.* **6**, 243–248. (doi:10.1175/1520-0469(1949)006<0243:TIVOFF>2.0.CO;2)
- Bussmann M, Chandra S, Mostaghimi J. 2000 Modeling the splash of a droplet impacting a solid surface. *Phys. Fluids* **12**, 3121. (doi:10.1063/1.1321258)
- Jepson W, Hickman J. 1993 *The Jepson manual: higher plants of California*. Berkeley, CA: University of California Press.
- McNaughton I, Harper J. 1964 Biological flora of the British Isles. Papaver I. *J. Ecol.* **52**, 767–793.
- Layne Z. 2007 Yellow flag iris. See <http://mtwow.org/yellow-flag-iris.html>.
- Davis C, Endress P, Baum D. 2008 The evolution of floral gigantism. *Curr. Opin. Plant Biol.* **11**, 49–57. (doi:10.1016/j.pbi.2007.11.003)
- Armstrong W. 2001 The world's smallest fruit. See <http://waynesword.palomar.edu/plfeb96.htm>.
- Orana. 2009 Rose hip (*Rosa canina* or *Rosa rugosa*). See <http://orana.eu/fruit.php?id=22>
- Ling D. 1999 *Commelina diffusa*. See [http://www.comfsm.fm/dleeling/botany/1999/vhp/commelina\\_diffusa.html](http://www.comfsm.fm/dleeling/botany/1999/vhp/commelina_diffusa.html).
- Plant-Life.org. Yellowbells: *Fritillaria pudica* (Pursh) Spreng. See [http://montana.plant-life.org/species/fritill\\_pudi.htm](http://montana.plant-life.org/species/fritill_pudi.htm).
- Club SRG. 2008 SRGV bulb log diary. See <http://www.srgc.org.uk/bulblog/log2008/040608/log.html>.
- Chayka K. 2006 *Chimaphila umbellata* (Pipsissewa). See <http://www.minnesotawildflowers.info/flower/pipsissewa>.
- Hilty J. 2011 Tumble mustard. See [http://www.illinoiswildflowers.info/weeds/weed\\_index.htm#tumble\\_mustard](http://www.illinoiswildflowers.info/weeds/weed_index.htm#tumble_mustard).
- Wax L. 1999 *Weeds of the North Central states*. Darby, PA: DIANE Publishing.
- Hilty J. 2011 Blue flag iris. See <http://www.illinoiswildflowers.info/wetland/plants/blueflag.htm>.
- Hedgerows, Hedges and Verges of Britain and Ireland. Hawthorn *Crataegus monogyna* and *C. levigata*. See <http://hedgerowmobile.com/hawthorn.html>.
- Weisenberger D. 2004 Yellow woodsorrel. See <http://www.agry.purdue.edu/turf/weeds/oxalis/oxalis.htm>.
- Schwartz D. 2005 Yellow wood sorrel. See <http://www.kingdomplantae.net/about.php>.
- Hedge N. 1994 *Erythrina variegata*—more than a pretty tree. See [http://www.winrock.org/fnrn/factnet/factpub/FACTSH/E\\_variegata.html](http://www.winrock.org/fnrn/factnet/factpub/FACTSH/E_variegata.html).
- Swearingen J, Remaley T. 2010 Chinese wisteria. See <http://www.nps.gov/plants/alien/fact/wisi1.htm>.
- Shokubutsuen D. 2010 *Trigonotis brevipes*. See [http://sigesplants.chicappa.jp/Trigonotis\\_brevipes.html](http://sigesplants.chicappa.jp/Trigonotis_brevipes.html).
- Kobayashi T. 2011 Tsumekusa summer flower. See <http://www.geocities.jp/nisi175812/tumekusa0.htm>.
- Yasou M. 2011 Hamatsumekusa. See <http://mikawanoyasou.org/data/hamatsumekusa.htm>.
- Ikeda Y. 2011 Nekonomesou no Nakama. See <http://yikflower.sakura.ne.jp/flower%20frame%20onekonomesou.html>.
- Okuyama Y. 2007 Charumerusou genus *Mitella* L. See <http://130.54.82.4/members/Okuyama/Msubram.html>.
- Office KE. 2008 Ocharumerusou no Kajitsu. See <http://granite.fc2web.com/amagi/html5/ocharmr3.html>.
- Brzeziecki B, Kienast F. 1994 Classifying the life-history strategies of trees on the basis of the Grimian model. *Forest Ecol. Manag.* **69**, 167–187. (doi:10.1016/0378-1127(94)-90227-5)
- Mazer S. 1989 Ecological, taxonomic, and life history correlates of seed mass among Indiana dune angiosperms. *Ecol. Monogr.* **59**, 153–175. (doi:10.2307/2937284)
- Forest Tree Seed Directory Food and Agriculture Organization of the United Nations. 1975 Food and Agriculture Organization Report. Rome, Italy: Food and Agriculture Organization of the United Nations.
- Grime J, Hodgson J, Hunt R. 1988 *Comparative plant ecology: a functional approach to common British species*. London, UK: Unwin Hyman Ltd.
- Michaels H *et al.* 1988 Seed size variation: magnitude, distribution, and ecological

- correlates. *Evol. Ecol.* **2**, 157–166. (doi:10.1007/BF02067274)
43. Aarssen L, Jordan C. 2001 Between-species patterns of covariation in plant size, seed size and fecundity in monocarpic herbs. *Ecoscience* **8**, 471–477.
  44. Lord J et al. 1997 Larger seeds in tropical floras: consistent patterns independent of growth form and dispersal mode. *J. Biogeogr.* **24**, 205–211. (doi:10.1046/j.1365-2699.1997.00126.x)
  45. Clifford H. 2000 Dicotyledon seedling morphology as a correlate of seed-size. In *Proc. of the Royal Society of Queensland*, vol. 109, pp. 39–48. Queensland, Australia: Royal Society of Queensland Inc.
  46. Jurado E, Westoby M, Nelson D. 1991 Diaspore weight, dispersal, growth form and perenniality of central Australian plants. *J. Ecol.* **79**, 811–828. (doi:10.2307/2260669)
  47. Carlowitz P. 1991 *Multipurpose trees and shrubs: sources of seeds and inoculants*. Nairobi, Kenya: International Council for Research in Agroforestry (ICRAF).
  48. O'Dowd D, Gill A. 1983 Seed dispersal syndromes in Australian *Acacia*. *Bull. Groupe Int. Etude Mimos* 52–55.
  49. Eriksson Å, Eriksson O. 1997 Seedling recruitment in semi-natural pastures: the effects of disturbance, seed size, phenology and seed bank. *Nordic J. Bot.* **17**, 469–482. (doi:10.1111/j.1756-1051.1997.tb00344.x)
  50. Cromarty A, Ellis R, Roberts E. 1982 *The design of seed storage facilities for genetic conservation international board for plant genetic resources*. Rome, Italy: IBPGR (International Board for Plant Genetic Resources).
  51. Schopmeyer C. 1974 *Seeds of woody plants in the United States US*. Washington, DC: Department of Agriculture Forest Service.
  52. Salisbury E. 1942 *The reproductive capacity of plants. Studies in quantitative biology*. London, UK: G. Bell.
  53. Grime J, Mason G, Curtis A, Rodman J, Band S. 1981 A comparative study of germination characteristics in a local flora. *J. Ecol.* **69**, 1017–1059. (doi:10.2307/2259651)
  54. Bouman F, Boesewinkel F, Bregman R, Deventer N, Oostermeijer J. 2000 *Verspreiding van zaden*. Zeist, Netherlands: KNNV Uitgeverij.
  55. Barclay A, Earle F. 1974 Chemical analyses of seeds iii oil and protein content of 1253 species. *Econ. Bot.* **28**, 178–236. (doi:10.1007/BF02861984)
  56. Earle F, Jones Q. 1962 Analyses of seed samples from 113 plant families. *Econ. Bot.* **16**, 221–250. (doi:10.1007/BF02860181)
  57. Thompson K, Bakker J, Bekker R. 1997 *The soil seed banks of North West Europe: methodology, density and longevity*, vol. 1. Cambridge, UK: Cambridge University Press.
  58. Pasandideh-Fard M, Qiao Y, Chandra S, Mostaghimi J. 1996 Capillary effects during droplet impact on a solid surface. *Phys. Fluids* **8**, 650. (doi:10.1063/1.868850)
  59. Chandra S, Avedisian C. 1991 On the collision of a droplet with a solid surface. *Proc. Math. Phys. Sci.* **432**, 13–41. (doi:10.1098/rspa.1991.0002)
  60. Šikalo Š, Tropea C, Ganić E. 2005 Impact of droplets onto inclined surfaces. *J. Colloid Interface Sci.* **286**, 661–669.
  61. Harlow F, Shannon J. 2009 The splash of a liquid drop. *J. Appl. Phys.* **38**, 3855–3866. (doi:10.1063/1.1709031)
  62. Brodie H. 1951 The splash-cup dispersal mechanism in plants. *Can. J. Bot.* **29**, 224–234. (doi:10.1139/b51-022)